

O/C and OM/OC Ratios of Primary, Secondary, and Ambient Organic Aerosols with High-Resolution Time-of-Flight Aerosol Mass Spectrometry

ALLISON C. AIKEN,^{†,‡}
 PETER F. DECARLO,^{†,§} JESSE H. KROLL,^{||}
 DOUGLAS R. WORSNOP,^{||}
 J. ALEX HUFFMAN,^{†,‡}
 KENNETH S. DOCHERTY,[‡]
 INGRID M. ULBRICH,^{†,‡}
 CLAUDIA MOHR,[‡] JOEL R. KIMMEL,[‡]
 DONNA SUEPER,[‡] YELE SUN,[⊥]
 QI ZHANG,[⊥] ACHIM TRIMBORN,^{||}
 MEGAN NORTHWAY,^{||} PAUL J. ZIEMANN,[#]
 MANJULA R. CANAGARATNA,^{||}
 TIMOTHY B. ONASCH,^{||}
 M. RAMI ALFARRA,[∇]
 ANDRE S. H. PREVOT, JOSEF DOMMEN,[∇]
 JONATHAN DUPLISSY,[∇] AXEL METZGER,[∇]
 JORS BALTEENSPERGER,[∇] AND
 JOSE L. JIMENEZ^{*,†,‡}

Department of Chemistry and Biochemistry, Cooperative Institute for Research in the Environmental Sciences (CIRES), and Department of Atmospheric and Oceanic Sciences (ATOC), University of Colorado at Boulder, 216 UCB, Boulder, Colorado 80309, Aerodyne Research Inc., Billerica, Massachusetts 01821, Atmospheric Sciences Research Center, State University of New York, Albany, New York 12222, Department of Environmental Sciences, University of California, Riverside, California 92521, and Laboratory of Atmospheric Chemistry, Paul Scherrer Institut, 5232 Villigen, Switzerland

Received December 3, 2007. Revised manuscript received February 26, 2008. Accepted February 27, 2008.

A recently developed method to rapidly quantify the elemental composition of bulk organic aerosols (OA) using a high-resolution time-of-flight aerosol mass spectrometer (HR-ToF-AMS) is improved and applied to ambient measurements. Atomic oxygen-to-carbon (O/C) ratios characterize the oxidation state of OA, and O/C from ambient urban OA ranges from 0.2 to 0.8 with a diurnal cycle that decreases with primary emissions and increases because of photochemical processing and secondary OA (SOA) production. Regional O/C approaches ~0.9. The hydrogen-to-carbon (H/C, 1.4–1.9) urban diurnal profile

increases with primary OA (POA) as does the nitrogen-to-carbon (N/C, ~0.02). Ambient organic-mass-to-organic-carbon ratios (OM/OC) are directly quantified and correlate well with O/C ($R^2 = 0.997$) for ambient OA because of low N/C. Ambient O/C and OM/OC have values consistent with those recently reported from other techniques. Positive matrix factorization applied to ambient OA identifies factors with distinct O/C and OM/OC trends. The highest O/C and OM/OC (1.0 and 2.5, respectively) are observed for aged ambient oxygenated OA, significantly exceeding values for traditional chamber SOA, while laboratory-produced primary biomass burning OA (BBOA) is similar to ambient BBOA, O/C of 0.3–0.4. Hydrocarbon-like OA (HOA), a surrogate for urban combustion POA, has the lowest O/C (0.06–0.10), similar to vehicle exhaust. An approximation for predicting O/C from unit mass resolution data is also presented.

Introduction

Atmospheric aerosols are important because of their effects on climate, health, visibility, and deposition to ecosystems and crops. Organic aerosols (OA) comprise a large fraction of the mass concentration of submicron particles (1). Primary OA (POA) is emitted directly as particles, whereas secondary OA (SOA) is formed in the atmosphere through chemical reactions that convert more volatile species into lower volatility products, which then partition to the particulate phase. The sources and composition of OA are uncertain, with current models underpredicting SOA by large factors in several recent studies (2). Because of the extreme range of properties (molecular weight, vapor pressure, polarity, etc.) of OA species, together with the chemical instability of some, typically only ~10% of the OA mass can be speciated (3). Because of this limitation, recent efforts have focused on methods that classify bulk OA by category (4–7).

Elemental analysis (EA) of bulk OA is of current interest because EA yields both the total organic mass and organic carbon. The most common measurement quantifies organic carbon (OC), which is typically multiplied by a constant conversion factor, an organic-mass-to-organic-carbon (OM/OC) ratio, to estimate OA total mass (8). A factor of 1.4 is traditionally used, although recent results support larger values (6, 9, 10), which are largely a function of the oxygen content. Measuring organic oxygen is also of interest because increasing oxygen content correlates with increasing density and water solubility of OA (8).

Traditional EA using commercial thermal techniques (11) is not applicable to rapid aerosol analysis because the large sample needed (1 mg) would require sampling for several hours under typical ambient concentrations (12). A thermal instrument, dedicated to the measurement of OA oxygen content, has been proposed (8), which could reduce sample needs and increase the time resolution but has not been demonstrated, to our knowledge. The nanoaerosol mass spectrometer (NAMS) (13) has recently demonstrated the ability to perform EA on individual particles of less than 10 nm in diameter. Particles are collected in an ion trap, followed by high-energy laser ablation that decomposes them into atomic ions, which are then detected with a time-of-flight mass spectrometer. Another method uses factor analysis of unit-mass resolution (UMR) mass spectra from the aerosol mass spectrometer (AMS) (14) to identify several components (5), allowing for the estimation of the elemental composition of each component (6), but the accuracy is limited by having to assume the elemental compositions of the ions.

* Corresponding author phone: (303) 492-3557; e-mail: jose.jimenez@colorado.edu.

[†] Department of Chemistry and Biochemistry, University of Colorado at Boulder.

[‡] Cooperative Institute for Research in the Environmental Sciences (CIRES), University of Colorado at Boulder.

[§] Department of Atmospheric and Oceanic Sciences (ATOC), University of Colorado at Boulder.

^{||} Aerodyne Research Inc.

[⊥] State University of New York.

[#] University of California.

[∇] Paul Scherrer Institut.

Recently, data from the high-resolution time-of-flight AMS (HR-ToF-AMS) have been used for EA of OA sampled in argon (12). In this paper, we improve the method for ambient measurements by presenting additional calibrations and addressing the interferences encountered while sampling in air. The advantages of this method are (1) very high time resolution, (2) online OA sampling reducing the possibility of artifacts, (3) requirement of ~ 6 orders of magnitude less sample than traditional techniques, and (4) use for samples including inorganic aerosol and OA, requiring no separation. The limitation is that it is not as accurate as traditional off-line analyses, which, however, do suffer from filter artifacts (e.g., adsorption, absorption, volatilization, reaction). The improved EA method is then applied to several source and ambient data sets to characterize and compare the elemental composition for different OA types. Last, we introduce an approximation that allows for the elemental composition of OA to be estimated from UMR AMS data sets.

Methods

EA with the HR-ToF-AMS. The HR-ToF-AMS has been described in detail previously (15) and improves upon previous versions of the AMS (14) by using a custom high-resolution TOFMS (Tofwerk). The TOFMS has two operating modes, utilizing two ion optical configurations, V and W modes. Because the W mode has the highest mass resolution (15), it is used whenever the data are not signal-limited; in this paper, this includes all spectra except the aircraft data. Mass spectra were acquired from m/z 10 to at least m/z 400 for all data, which was analyzed in Igor Pro 5.0 (Wavemetrics, Lake Oswego, OR) using the standard ToF-AMS data analysis program, the additional HR-ToF-AMS analysis software program (Pika) (15), and custom analysis routines for EA (12).

Because the theory and initial application of EA to HR-ToF-AMS data has been previously described (12), only a short description follows. The ion current in electron ionization mass spectrometry is approximately proportional to the mass concentration present in the ionization region for molecules composed of small atoms (16). Therefore, the same ion current at different m/z 's represents the same original mass, allowing for the average composition of the ions to be calculated (12). For a complex spectrum of an unknown species or mixture, the best approximation of the elemental composition of the original species is the averaged ion composition across the mass spectrum. Raw measured atomic ratios for oxygen-to-carbon (O/C), hydrogen-to-carbon (H/C), and nitrogen-to-carbon (N/C) are converted to estimated ratios using calibration factors, determined by sampling standards. Estimated atomic ratios are used to calculate OM/OC (12).

HR-ToF-AMS Data Collection. All laboratory aerosol standards were produced by atomizing aqueous or organic (isopropyl alcohol or ethyl acetate) solution. The aerosol was dried using multiple diffusion driers filled with silica gel or activated carbon, depending on the solvent, to remove excess solvent. Three main types of laboratory standards were studied: individual standards previously identified in aerosols, amino acids, and fulvic acids (FAs). References and details for all samples can be found in Table S-1 (Supporting Information). The 35 compounds in the first group were atomized from organic solutions (12). A total of 20 amino acids (17) (from Sigma-Aldrich) and 4 FA samples [from the International Humic Substances Society (IHSS)] (18) were sampled from aqueous solution. All particles were generated in prepurified argon, except the amino acids that were collected under purified dry air. Reference atomic ratios for the FA samples were measured by standard EA techniques for the IHSS (18).

Ambient data were acquired in the greater Mexico City area during the MILAGRO (Megacity Initiative: Local and

Global Research Observations) field campaign in March 2006. Ground-based data are from the T0 Supersite at the Instituto Mexicano del Petr leo (IMP), and aircraft data are from the NCAR C-130 collected during two flights that overflew Mexico City (19). Both data sets were analyzed using positive matrix factorization (PMF) (20, 21), yielding high-resolution mass spectra of four previously identified major components (5, 6, 21): (a) hydrocarbon-like OA (HOA), a surrogate of primary combustion OA; (b and c) two types of oxygenated OA, OOA-I and OOA-II, previously characterized as surrogates for "aged" and "fresher" SOA, respectively; (d) a biomass burning OA (BBOA). Component spectra were analyzed by EA.

Chamber SOA (C-SOA) was generated in either a $\sim 6.6\text{-m}^3$ poly(tetrafluoroethylene) environmental chamber at the University of California—Riverside (UCR) or a 27-m^3 hexafluoropropylene—tetrafluoroethylene copolymer (FEP) chamber at the Paul Scherrer Institut (PSI), Villigen, Switzerland. Data are presented from three UCR experiments conducted under dry conditions ($\sim 0\%$ RH): (1) 2 ppm α -pinene + ~ 2 ppm ozone and photooxidations with OH (from ~ 20 ppb methyl nitrite) of (2) 300 ppb toluene and (3) ~ 1 ppm gasoline vapors (both under 200 ppb NO) that yielded ~ 500 , 90, and $60 \mu\text{g}/\text{m}^3$ OA, respectively. Three additional photooxidation experiments were conducted at PSI under $\sim 50\%$ relative humidity (RH): (4) 240 ppb α -pinene with 120 ppb NO_x , (5) ~ 1.3 ppm isoprene with 600 ppb NO_x , and (6) 1.2 ppm trimethylbenzene with 600 ppb NO, yielding 100, 60, and $50 \mu\text{g}/\text{m}^3$ OA. The concentration levels and systems used were chosen because they have been previously studied and used in SOA modeling (e.g., (22)).

Laboratory-produced primary biomass burning OA (P-BBOA) was sampled during FLAME-1 (Fire Laboratory at Missoula Experiment, phase 1) in June 2006 at the United States Department of Agriculture (USDA) Missoula Fire Sciences Laboratory (Missoula, MT). Results from burns of two samples are presented because they span the range of mass spectra, volatility, and combustion conditions observed during FLAME-1. Samples of ~ 200 g of lodgepole pine and a combination of sage and rabbitbrush were separately subjected to open-air combustion inside a large chamber ($\sim 3700 \text{ m}^3$) with vigorous fan mixing at room temperature, allowing for dilution of $\sim 10^4$ before being sampled by the HR-ToF-AMS. Combustion particles sampled were a mixture of both flaming and smoldering aerosol produced from each biomass.

Additional POA was generated from vehicle emissions using a diesel and a gasoline vehicle. The vehicles were operated by briefly revving the engines inside a 240-m^3 shed in a rural area outside Boulder, CO, where the exhaust was diluted at least by a factor of 100 and sampled for ~ 20 min while its concentration was further diluted by infiltration of ambient air with a much lower OA concentration.

Results and Discussion

Improvement of EA Method Calibration for Ambient Measurements. We have shown previously that the raw measurement of organic O/C tends to be biased low because of the influence of unimolecular ion decomposition reactions, in which a fragment with an electronegative atom such as oxygen has a larger tendency to become a neutral, rather than a cation (12). Previous calibrations using laboratory standards show that the bias can be accounted for in an average sense (12). N/C and especially H/C showed less bias than O/C. The initial calibrations were designed to establish the viability of the method, but the inclusion of additional standards in the calibration is desirable. Most of the initial standards have spectra more similar to HOA rather than OOA, which could bias the calibrations. This similarity is not surprising because at least 16 of the standards were first

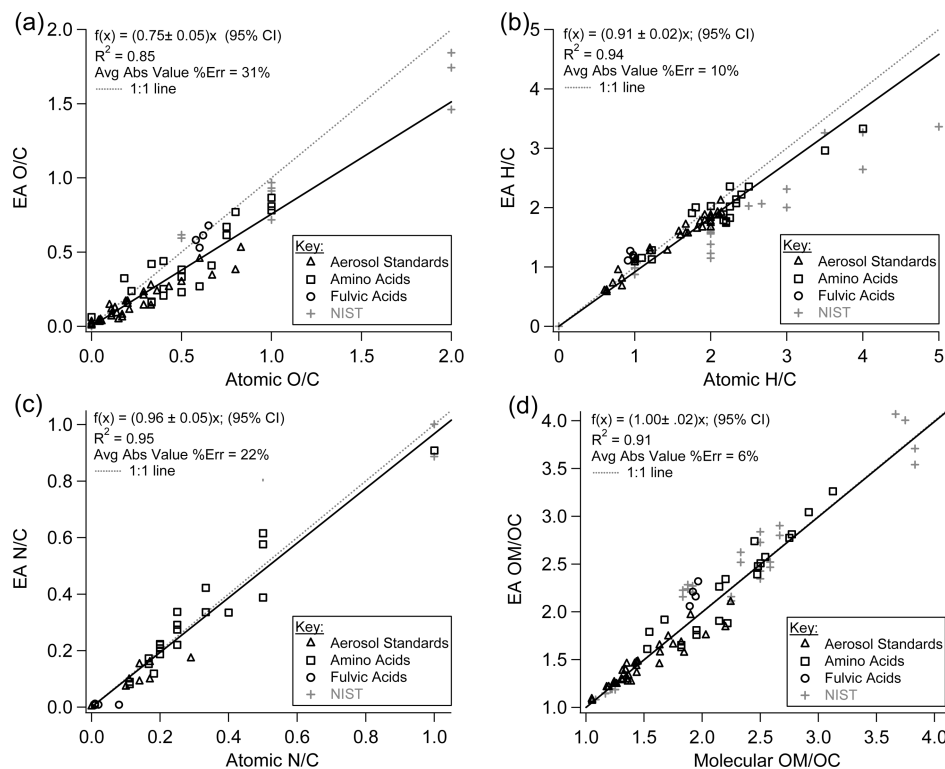


FIGURE 1. (a–c) Atomic ratios (a, O/C; b, H/C; c, N/C) of organic signals from laboratory standards versus nominal ratios, used to calibrate our EA method with linear regressions through zero. (NIST data are shown for visual reference and are not used in the calibrations.) (d) Mass ratio OM/OC calculated from calibrated atomic ratios. (Table S-1 in the Supporting Information details the standards used.)

identified in ambient POA (23). The spectra of most of the standards are dominated by $C_xH_y^+$ ions, and most do not have large CO_2^+ (m/z 44) signals, with the exception of the dicarboxylic acids and acyl peroxides, while ambient OA spectra often have a large CO_2^+ signal when OOA is significant. Also of note, carboxylic acids produced significant signals at m/z 60 and 73, specifically $C_2H_4O_2^+$ and $C_3H_5O_2^+$, fragments that are also associated with nonacid BBOA markers such as levoglucosan. For these reasons, additional calibrations were performed, including standards of different chemical types such as FAs, soil-derived water-soluble humic acid extracts that have been proposed as surrogates for aged oxygenated OA (5, 7), and amino acids and amino compounds, which have been observed in significant concentrations in fine particles (24) and represent a complex mixed-functionality type of molecule that was not explored in the previous calibrations. Although FAs are used as surrogates for oxidized/aged OA, the OM/OC of FAs measured by standard EA (1.90 ± 0.02) (18) are less than that proposed for oxidized OA by Turpin and Lim (2.1 ± 0.2) (10). Also, the retention of significant strongly bound molecular water by the hygroscopic FA standards has been reported as a problem for traditional EA of these standards (25). Because FAs are empirically defined based on their water solubility, the EA analyses conducted in this paper used water as the solvent for atomization prior to the HR-ToF-AMS measurements to avoid fractionation that could occur when atomizing in organic solvents. Because fragmentation of organic species produces H_2O^+ ions, which are not distinguishable from molecular water, in the absence of further information, half of the FA water signal was used in the determination of their EA, and the other half was considered to arise from the ionization of strongly bound molecular water. Table S-2 in the Supporting Information presents a sensitivity analysis for this assumption, indicating that the resulting uncertainty in the calibration slopes is an order of magnitude less than the uncertainty/error of the EA method.

The new calibration plots are shown in Figure 1a–c. The resulting calibrations were used to calculate OM/OC values, which are compared with the actual values in Figure 1d. As in the previous results with fewer compounds (12), the largest negative bias in the raw atomic ratios is for O/C, with a linear regression slope of 0.75 ($R^2 = 0.85$). The uncertainty, defined before as the average absolute value of the relative error of each data point with respect to the regression line (12), is 31%. Precision is much better than accuracy for individual compounds at $\pm 3\%$, indicating that the variability in the bias from molecule to molecule is the dominant contribution to the uncertainty. Because this uncertainty is an average of single standards, we expect that it should be an upper limit for the uncertainty when measuring complex mixtures, such as ambient OA, because of compensating effects from different compounds. The H/C measurements have a much smaller bias with a slope of 0.91 ($R^2 = 0.94$) and lower average uncertainty, 10%. The H/C bias for the NIST data is greater than that for the AMS standards, for reasons discussed previously (12). N/C has the least average bias, slope of 0.96 ($R^2 = 0.95$), with an uncertainty of 22%. The reconstruction of OM/OC values from the calibrated atomic ratios has an average error of 6%. FA data have a less negative bias for our EA, which may be partially due to remaining strongly bound molecular water, which is more likely to be included in our method (based on atomization of water solutions) than traditional EA.

Correcting for Interferences in Ambient Air. The calibrations discussed above involve standards, and most were performed under argon. When sampling ambient particles, significant interferences arise from gas-phase species and from other particulate species, which can require additional corrections. The AMS inlet concentrates particles relative to the gas phase by a factor of 10^7 . However, there is still a significant signal from the major gas-phase species (N_2 , O_2 , Ar, H_2O , and CO_2), which can complicate the analysis of the particulate spectrum. Signals from incompletely dried par-

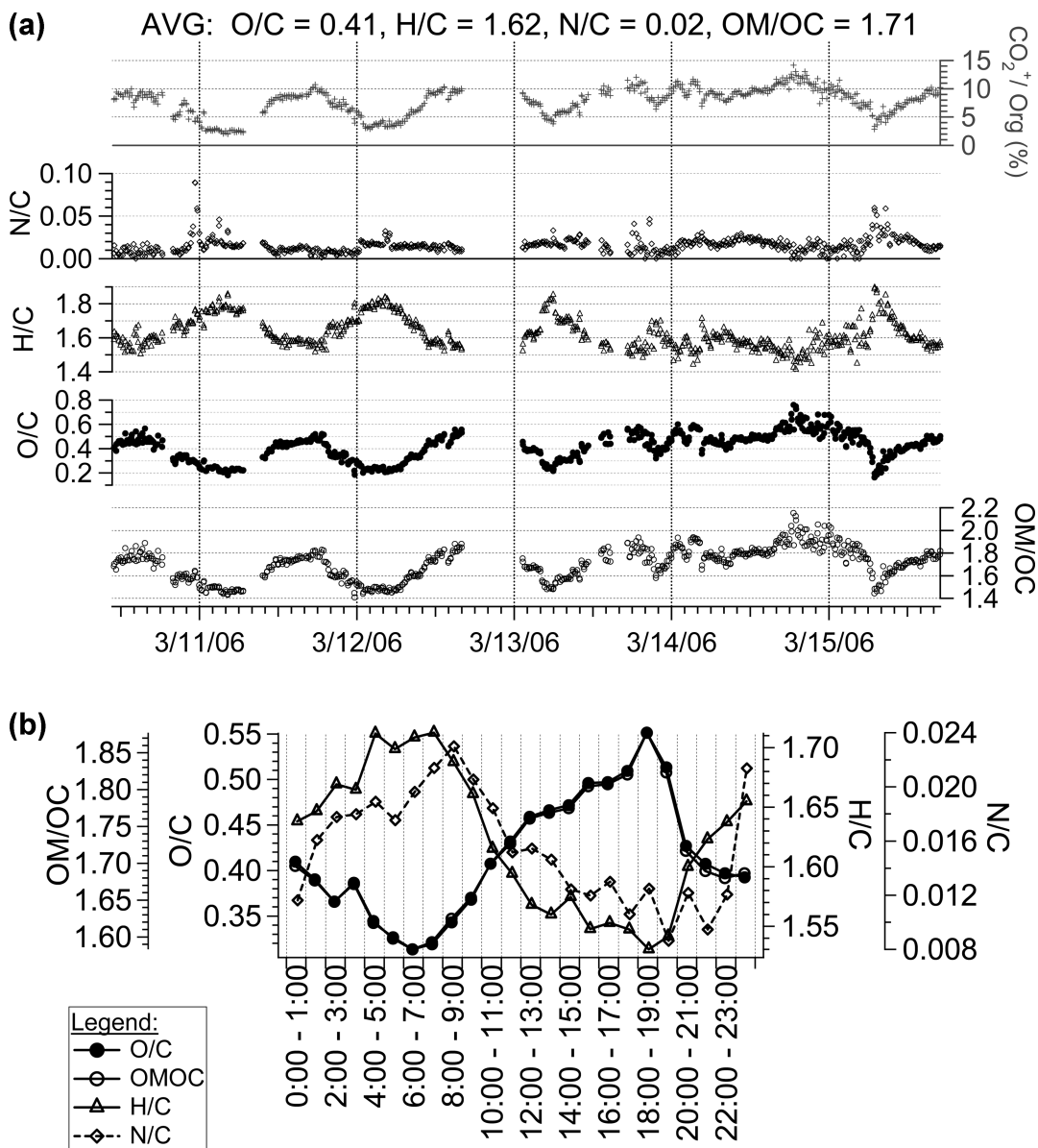


FIGURE 2. (a) Time series and (b) diurnal averages of atomic O/C, H/C, N/C, and OM/OC sampled at the ground site in Mexico City.

ticles and/or gas-phase water occur at H_2O^+ , OH^+ , and O^+ (H_xO^+ for short), which are also produced from OA. Ambient sampling with the AMS is typically done with a dryer to remove most particle-phase water. However, drying is often not complete, and significant gas-phase H_xO^+ and sometimes strongly bound particle-phase H_xO^+ remain. Sulfate aerosols also produce a significant signal at H_xO^+ , which is not directly separable from the OA or particulate water signals.

Accurately determining the OA signal at CO^+ is also difficult. The interference from $\text{CO}(\text{g})$ is negligible except perhaps when sampling concentrated combustion exhaust, but the very large signal at N_2^+ from $\text{N}_2(\text{g})$ can overwhelm the spectrum at m/z 28, resulting in an inaccurate quantification of particulate CO^+ due to the finite resolution of the spectrometer (15).

Several techniques can be applied to reduce or quantify the interferences to CO^+ and H_xO^+ when sampling ambient aerosols. AMS measurements of HEPA-filtered ambient air are always taken intermittently and used with the HR-ToF-AMS to calibrate the air signals; however, the signal from air at N_2^+ is very large, and this subtraction is typically not precise enough to allow direct determination of CO^+ except when sampling highly concentrated aerosols, e.g.,

source measurements, or when long averaging times can be used. The organic signal at CO^+ can be estimated from the particle time-of-flight (PToF) mode signal (5), and although this typically requires significant averaging, the organic m/z 28/44 ratio has been quantified with this technique in two studies from Pittsburgh and Tokyo (5, 26). The response of the AMS to gas-phase H_xO^+ can be measured when sampling through a filter, and together with a continuous RH measurement, it can be used to remove this contribution from an ambient data set. H_xO^+ ions from particulate water can be minimized by drying the sample before entering the AMS, as mentioned above. The contribution of sulfates to H_xO^+ can be estimated from laboratory calibrations and removed using the fragmentation table in the AMS software (27). A more elaborate setup could be used in which the aerosols could be sampled into an argon flow using a counterflow virtual impactor, which would facilitate the measurement of CO^+ and H_xO^+ from ambient organics by removing most of the interfering signals (although the sulfate H_2O^+ interference would remain). However, this technique may cause losses of smaller particles and semivolatile species, which could alter the O/C ratio of the sampled aerosol because more

oxygenated species tend to be less volatile (28). Future ambient and chamber studies should make an effort to quantify the contribution of organic species to the H_xO^+ and CO^+ signals. The data presented here used filters and PToF data to constrain the CO^+ and H_xO^+ signals whenever possible. We also used the increase in the signal at m/z 28 with organic mass for ambient measurements to estimate the CO^+ signal as a function of the CO_2^+ signal. Both ground and aircraft data indicate a ratio of ~ 1 for CO^+/CO_2^+ OA using this method.

The accuracy of the EA method could be further improved by calibrating measured O/C's from the HR-ToF-AMS with the results of traditional EA done on filters collected for the same sample. However, because of the requirements for traditional EA, these calibrations are more practical for laboratory and chamber applications than ambient samples because of the comparatively large sample size (1 mg) required for traditional analysis, as mentioned before. Care should be taken to minimize artifacts due to adsorption or evaporation from filters, which would introduce differences in the O/C ratios of the filter sample from what the AMS sampled in parallel.

Improved Fragmentation Table for Ambient Organics.

In order to quantify organic particle mass and elemental composition, the organic contribution to H_xO^+ and CO^+ signals needs to be estimated. In practice, most studies apply a "fragmentation table" (27). The "standard" fragmentation table in use to date estimates the H_2O^+ signal as equal to the CO_2^+ signal based on early calibrations with dicarboxylic acids (Silva, P., unpublished data). The OH^+ signal is estimated at 25% of H_2O^+ and the O^+ as 4% of the H_2O^+ signal, based on AMS water fragmentation measurements, which can be verified for each instrument using background signals that have little uncertainty and are supported by the laboratory data included here. The organic signal at CO^+ is neglected in the standard table.

We propose to implement a new fragmentation table that is consistent with currently available information. Because the standard fragmentation table results in good agreement with other aerosol measurements (6, 9, 14), any changes to it should not alter the total organic mass. The CO^+ signal has been estimated to be ~ 0.9 – 1.25 times the CO_2^+ signal during four ambient campaigns (5, 19, 26), and the organic H_xO^+ signal is smaller than the CO^+ signal for the laboratory standards and C-SOA measured here and elsewhere (Shilling, J. Personal communication, Harvard University, 2007) (26). Thus, it appears that the organic H_xO^+ signal is overestimated in the standard fragmentation table, while the CO^+ signal is underestimated. If the standard table is applied before EA of ambient or chamber data, it will result in a positive bias of the O/C and H/C ratios. Therefore, we propose the use of the following fragmentation patterns in relation to measured CO_2^+ signals when they cannot be constrained by other methods: $CO^+ = 100\%$, $H_2O^+ = 22.5\%$, $OH^+ = 5.625\%$ (25% of H_2O^+), $O^+ = 0.90\%$ (4% of H_2O^+). Changes from the standard AMS fragmentation table are included in Table S-3 in the Supporting Information. As further information becomes available on these relative intensities from more field and laboratory studies, it may be desirable to further update the fragmentation table or to develop alternative formulations for specific OA types. Clearly, when compared to the application of EA to spectra of species analyzed in argon, ambient measurements with these predicted fragmentation patterns will have a larger uncertainty.

Remaining Uncertainties. Variations in the bounce-related collection efficiency (E_b) (5) or in the relative ionization efficiency (16) of different types of organic species are possible and could cause additional biases in the O/C ratio of total organics reported with our OA technique. Both of these potential biases would likely tend to reduce the signal from

oxygenated species relative to reduced species (5, 16) and thus result in an underestimation of O/C. The quantification of these potential differences should be a subject of future research. Short of quantifying these differences, a good approach is to separately quantify the O/C ratios of the various PMF OA components and then acknowledge the potential biases when reporting O/C for total organics. An additional source for O/C and N/C underquantification is related to organonitrates and organosulfates because they could form ions nominally considered to be inorganic. Although we expect these biases to be small because during most ambient campaigns the large majority of the inorganic ions are indeed from inorganic species, this should be a subject of future research (12). (Table S-4 in the Supporting Information includes the potential effects.)

Application of EA to Ambient OA and POA and SOA

Sources. Organic EA was applied to ambient urban OA sampled over a period of 6 days during MILAGRO at the T0 ground site in Mexico City. Elemental mass signals averaged from this period are shown in Figure S-1 in the Supporting Information. From the elemental signals, dominance of carbon and oxygen in OA mass is unequivocal. Time series of O/C, H/C, N/C, and OM/OC are shown in Figure 2a. The precision of the method for ambient measurements is clear from the time series of the ratios for these 2.5 min data and, as for the laboratory measurements, is much higher than the nominal accuracy. Also plotted is the percentage of the total organic signal at CO_2^+ , which has a good correlation with the O/C ratio. This supports the use of CO_2^+/OA (or m/z 44/OA in UMR data) as a qualitative indicator of the O/C ratio; the quantitative relationship is explored in more detail below. The averages over this period were O/C = 0.41 (range 0.16–0.76), H/C = 1.62 (1.41–1.89), N/C = 0.02 (0.00–0.09), and OM/OC = 1.71 (1.41–2.15). Note that OM/OC values are larger than the value of 1.4 that was used for many years to calculate OM from OC and are consistent with the range of results from other techniques (6, 9, 10).

The estimated N/C is an order of magnitude lower than O/C, highlighting the dominance of oxygen among organic heteroatoms in urban OA. For this reason, OM/OC is highly correlated with O/C, as was hypothesized by Pang et al. (8). The reported N/C could have a small negative bias because it does not include any nitrogen that would be from "nominally inorganic fragments" in the AMS, such as NH_x^+ or NO_x^+ fragments from species such as organic nitrates or amines. This would also negatively bias O/C and H/C. However, the majority of the nominally inorganic ions appear to originate from inorganic species because the balance of the measured anions with ammonium appears to be achieved within the accuracy of the measurements for this campaign. Thus, fragments of organic origin are not likely to be a large portion of these ions, and their contributions are expected to be at most on the order of the scatter of the ammonium balance. Nominally, less than 10% of the total nitrogen sampled is from nitrogen atoms in organic compounds, with >90% of the nitrogen being present as ammonium and nitrate. Additional calibrations should be carried out, especially for organic nitrates, in order to determine the percentage of the nitrogen signal appearing at organic versus nominally inorganic fragment ions. For the T0 data presented here, some early mornings have enhanced N/C, likely from a more local source due to their short time periods.

Figure 2b shows 1-h diurnal averages. H/C is the highest during the early morning because of a higher influence of HOA and primary BBOA emissions during that time period and lowest in the afternoon when SOA is most important. N/C has a similar profile, indicating that a significant fraction of the N in OA is likely associated with POA in this study. O/C and OM/OC increase later in the day, as would be expected

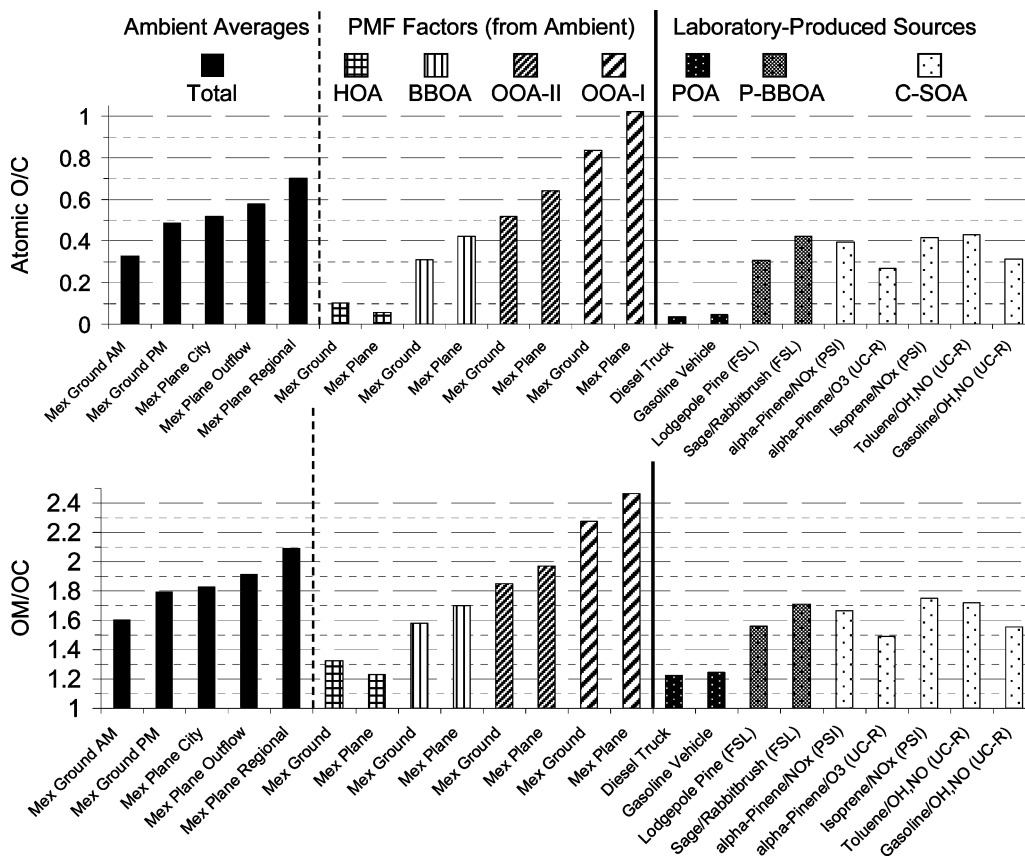


FIGURE 3. (a) O/C and (b) OM/OC for ambient aerosols in Mexico City, PMF components from analysis of Mexico City data, and chamber and laboratory sources of OA. Average ground OA AM and PM are from local 4–9 a.m. and 1–6 p.m., respectively.

from SOA formation associated with the increased photochemistry in the afternoon in Mexico City (2).

Figure 3 compares O/C and OM/OC values from different POA and SOA sources, ambient OA, and components from PMF analysis of ambient OA. Because O/C and OM/OC are highly correlated, we will only refer to O/C in the following discussion. The averaged morning spectrum from MILAGRO has the lowest values from all of the ambient averages sampled either at the ground site or from the aircraft, consistent with the largest fraction of POA expected at this location and time. O/C increases for the afternoon ground average as expected based on increased photochemistry and SOA formation, with further increases for the aircraft averages above the city and downwind of the city, indicating the strong influence of additional SOA formation and processing, consistent with previous results from Mexico City (2, 19). The regional background average O/C value further indicates this trend of increasing O/C with increased processing time or “age”.

Applying PMF to the ground and aircraft data results in four main components for both data sets. The mass spectra and the O/C of the PMF factors from the ground site and the aircraft are similar although not identical. HOA has the lowest O/C at 0.06–0.10, indicating a small oxygen content present within this factor associated with primary emissions that is consistent with NAMS results (29). O/C from HOA is very similar to that from POA sampled from diesel and gasoline exhaust, 0.03 and 0.04, respectively. BBOA has O/C of 0.31 near the ground increasing to 0.42 in the aircraft, potentially due to SOA formation and processing from BB precursors, which would have a higher influence in the more aged BB air masses sampled by aircraft. OOA-II, interpreted previously as fresh urban SOA, has O/C ~ 0.52–0.64, consistent with NAMS measurements of freshly produced ambient SOA (29) and

again higher in the aircraft presumably because of increased aging. Finally, OOA-I, interpreted as aged regional OA, has the largest O/C (range 0.83–1.02) from any factors or sources studied to date and again increased for the more aged air masses.

C-SOA from various precursors at relatively high concentrations have intermediate O/C values (range 0.27–0.43), similar to results from biogenic SOA produced in flow tubes measured with the NAMS (30). C-SOA O/C values are comparable to, but lower than, the OOA-II factors from PMF, consistent with the fact that the ratio of $C_2H_3O^+$ (at m/z 43) to CO_2^+ (at m/z 44) is larger for C-SOA. This suggests that C-SOA is less oxidized than fresher ambient OOA. Ambient OOA-I is dominated by CO_2^+ and is significantly more oxidized than OOA-II and the C-SOA sampled here. C-SOA produced at lower concentrations (more relevant to the ambient atmosphere) tends to have increased O/C, closer to that of ambient OOA (31). The O/C of laboratory-produced P-BBOA is similar to those observed for the ground BBOA factor. All BBOA analyzed here have OM/OC (1.56–1.70) values lower than those calculated by Turpin and Lim for fireplace combustion (~2.0) (10), possibly because of the different fuels and/or conditions of combustion and sampling. However, the trend of both analyses is consistent with OM/OC values for POA < BBOA < OOA.

Figure 4a shows that there is a direct correlation between the O/C and OM/OC for all of the data presented here. The y intercept from fitting of the ambient data is close to the value for CH_3 (OM/OC = 1.25, O/C = 0), and the linear regression reaches OM/OC = 2.44 with O/C = 1.0, which could be ascribed to an empirical formula of $CH_{1.3}O$.

Approximation of O/C for UMR Data. Prior to the present work, many authors have used the fraction of the organic signal at m/z 44 as a surrogate for the relative oxygen

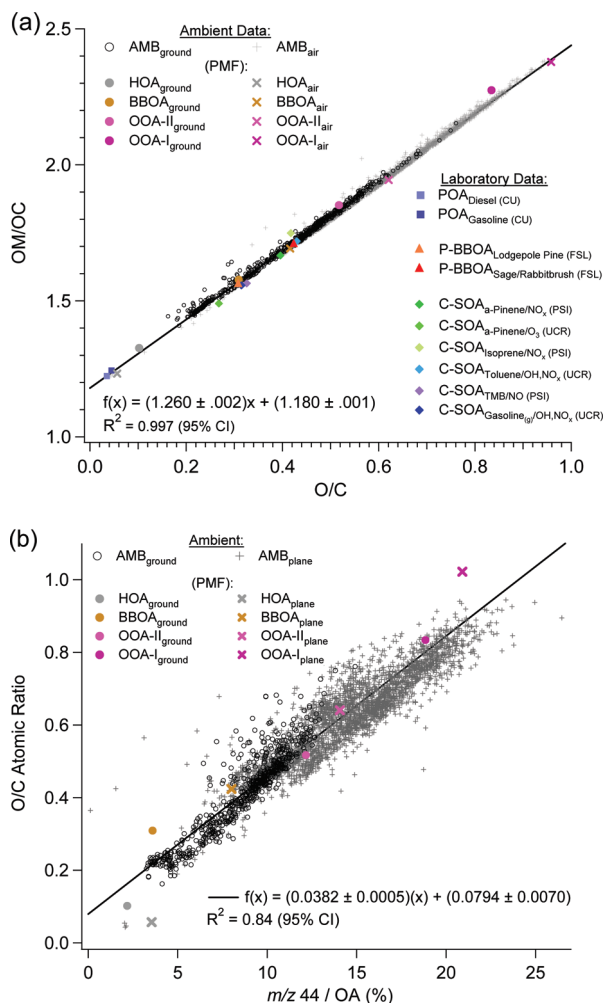


FIGURE 4. (a) Scatter plot of OM/OC vs O/C for all ambient and chamber OA. (b) Scatter plot of m/z 44/OA vs. O/C from UMR data with a 9% error (average absolute value of the relative error), when fit by linear regression and weighting ground and aircraft data equally.

content of the OA because m/z 44 was considered to be dominated by CO_2^+ in ambient OA, based on sampling of dicarboxylic acids in the laboratory. With the HR-ToF-AMS, the dominance of CO_2^+ in the signal at m/z 44 becomes unequivocal, and, e.g., in the T0 data, CO_2^+ was an average of 88% ($\pm 8.2\%$, 1 standard deviation) of m/z 44. Figure S-2 in the Supporting Information plots CO_2^+ /OA vs O/C. Figure 4b shows that O/C and m/z 44 have significant correlation. This justifies the use of m/z 44 as a surrogate for the oxygen content of OA in data sets in which only UMR AMS data are available.

Acknowledgments

This research was supported by grants from the NSF (Grants ATM-0449815 and ATM-0513116), the U.S. Department of Energy's Atmospheric Science Program (Office of Science, BER; Grant DE-FG02-05ER63981), EPA (Grants STAR-RD-83216101-0 and STAR-RD-83108001, and Fellowship FP-91650801), NASA (Grants NNG04GA67G and NNG06GB03G and ESS Graduate Fellowships NNG04GR06H, NGT5-30516, and NNG05GQ50H), and EC (Grants EUROCHAMP FP6-505968). Any opinions or findings are those of the authors and do not reflect the views of the funding agencies. We thank Dara Salcedo, and Michael Hannigan for assistance in data collection, Luisa Molina and Sasha Madronich for organizing MILAGRO, Sonia Kreidenweis, Cyle Wold, Wei-

Min Hao, and Bill Malm for organizing FLAME-1, and Aerodyne, Tofwerk, and the rest of the Jimenez Group for technical support and useful discussions.

Supporting Information Available

Four tables and two figures, mentioned in the text. This material is available free of charge via the Internet at <http://pubs.acs.org>.

Literature Cited

- Zhang, Q.; Jimenez, J. L.; Canagaratna, M. R.; Allan, J. D.; Coe, H.; Ulbrich, I. M.; Alfarra, M. R.; Takami, A.; Middlebrook, A. M.; Sun, Y. L.; Dzepina, K.; Dunlea, E.; Docherty, K.; DeCarlo, P. F.; Salcedo, D.; Onasch, T. B.; Jayne, J. T.; Miyoshi, T.; Shimojo, A.; Hatakeyama, S.; Takegawa, N.; Kondo, Y.; Schneider, J.; Drewnick, F.; Borrmann, S. L.; Weimer, S.; Demerjian, K.; Williams, P.; Bower, K. N.; Behreini, R.; Cottrell, L.; Griffin, R. J.; Rautiainen, J.; Sun, J. Y.; Zhang, Y. M.; Worsnop, D. R. Ubiquity and dominance of oxygenated species in organic aerosols in anthropogenically-influenced northern hemisphere mid-latitudes. *Geophys. Res. Lett.* **2007**, *34* (13), L13801; doi:10.1029/2007GL029979.
- Volkamer, R.; Jimenez, J. L.; San Martini, F.; Dzepina, K.; Zhang, Q.; Salcedo, D.; Molina, L. T.; Worsnop, D. R.; Molina, M. J. Secondary organic aerosol formation from anthropogenic air pollution: Rapid and higher than expected. *Geophys. Res. Lett.* **2006**, *33* (17), L17811.
- Rogge, W. F.; Mazurek, M. A.; Hildemann, L. M.; Cass, G. R.; Simoneit, B. R. T. Quantification of urban organic aerosols at a molecular-level—identification, abundance and seasonal-variation. *Atmos. Environ., Part A* **1993**, *27* (8), 1309–1330.
- Blando, J. D.; Porcja, R. J.; Li, T. H.; Bowman, D.; Lioy, P. J.; Turpin, B. J. Secondary formation and the smoky mountain organic aerosol: An examination of aerosol polarity and functional group composition during SEAVS. *Environ. Sci. Technol.* **1998**, *32* (5), 604–613.
- Zhang, Q.; Alfarra, M. R.; Worsnop, D. R.; Allan, J. D.; Coe, H.; Canagaratna, M. R.; Jimenez, J. L. Deconvolution and quantification of hydrocarbon-like and oxygenated organic aerosols based on aerosol mass spectrometry. *Environ. Sci. Technol.* **2005**, *39* (13), 4938–4952.
- Zhang, Q.; Worsnop, D. R.; Canagaratna, M. R.; Jimenez, J. L. Hydrocarbon-like and oxygenated organic aerosols in Pittsburgh: Insights into sources and processes of organic aerosols. *Atmos. Chem. Phys.* **2005**, *5*, 3289–3311.
- Decesari, S.; Facchini, M. C.; Matta, E.; Mircea, M.; Fuzzi, S.; Chughtai, A. R.; Smith, D. M. Water soluble organic compounds formed by oxidation of soot. *Atmos. Environ.* **2002**, *36* (11), 1827–1832.
- Pang, Y.; Turpin, B. J.; Gundel, L. A. On the importance of organic oxygen for understanding organic aerosol particles. *Aerosol Sci. Technol.* **2006**, *40* (2), 128–133.
- Takegawa, N.; Miyazaki, Y.; Kondo, Y.; Komazaki, Y.; Miyakawa, T.; Jimenez, J. L.; Jayne, J. T.; Worsnop, D. R.; Allan, J. D.; Weber, R. J. Characterization of an aerodyne aerosol mass spectrometer (AMS): Intercomparison with other aerosol instruments. *Aerosol Sci. Technol.* **2005**, *39* (8), 760–770.
- Turpin, B. J.; Lim, H. J. Species contributions to PM_{2.5} mass concentrations: Revisiting common assumptions for estimating organic mass. *Aerosol Sci. Technol.* **2001**, *35* (1), 602–610.
- Ma, T. S.; Wang, C. Y.; Gutterson, M. Organic elemental analysis. *Anal. Chem.* **1982**, *54* (5), R87–R96.
- Aiken, A. C.; DeCarlo, P. F.; Jimenez, J. L. Elemental analysis of organic species with electron ionization high-resolution mass spectrometry. *Anal. Chem.* **2007**, *79* (21), 8350–8358.
- Wang, S. Y.; Zordan, C. A.; Johnston, M. V. Chemical characterization of individual, airborne sub-10-nm particles and molecules. *Anal. Chem.* **2006**, *78* (6), 1750–1754.
- Canagaratna, M. R.; Jayne, J. T.; Jimenez, J. L.; Allan, J. D.; Alfarra, M. R.; Zhang, Q.; Onasch, T. B.; Drewnick, F.; Coe, H.; Middlebrook, A.; Delia, A.; Williams, L. R.; Trimborn, A. M.; Northway, M. J.; DeCarlo, P. F.; Kolb, C. E.; Davidovits, P.; Worsnop, D. R. Chemical and microphysical characterization of ambient aerosols with the aerodyne aerosol mass spectrometer. *Mass Spectrom. Rev.* **2007**, *26* (2), 185–222.
- DeCarlo, P. F.; Kimmel, J. R.; Trimborn, A.; Northway, M. J.; Jayne, J. T.; Aiken, A. C.; Gonin, M.; Fuhrer, K.; Horvath, T.; Docherty, K. S.; Worsnop, D. R.; Jimenez, J. L. Field-deployable, high-resolution, time-of-flight aerosol mass spectrometer. *Anal. Chem.* **2006**, *78* (24), 8281–8289.

- (16) Jimenez, J. L.; Jayne, J. T.; Shi, Q.; Kolb, C. E.; Worsnop, D. R.; Yourshaw, I.; Seinfeld, J. H.; Flagan, R. C.; Zhang, X. F.; Smith, K. A.; Morris, J. W.; Davidovits, P. Ambient aerosol sampling using the aerodyne aerosol mass spectrometer *J. Geophys. Res., [Atmos.]* **2003**, *108* (D7), 8425; doi: 8410.1029/2001JD001213.
- (17) Sun, Y.; Zhang, Q. Bulk characterization and quantification of organic nitrogen species in atmospheric condensed phases based on high resolution time-of-flight aerosol mass spectrometry. *Environ. Sci. Technol.* 2008, in preparation.
- (18) <http://www.ihss.gatech.edu/>.
- (19) DeCarlo, P. F.; Dunlea, E. J.; Kimmel, J. R.; Aiken, A. C.; Sueper, D.; Crouse, J.; Wennberg, P. O.; Emmons, L.; Shinozuka, Y.; Clarke, A.; Zhou, J.; Tomlinson, J.; Collins, D.; Knapp, D.; Weinheimer, A.; Campos, T.; Jimenez, J. L. Fast airborne aerosol size and chemistry measurements with the high resolution aerosol mass spectrometer during the MILAGRO campaign. *Atmos. Chem. Phys. Discuss.* **2007**, *7*, 18269–18317.
- (20) Paatero, P.; Tapper, U. Positive matrix factorization—a non-negative factor model with optimal utilization of error-estimates of data values. *Environmetrics* **1994**, *5* (2), 111–126.
- (21) Lanz, V. A.; Alfarra, M. R.; Baltensperger, U.; Buchmann, B.; Hueglin, C.; Prevot, A. S. H. Source apportionment of submicron organic aerosols at an urban site by factor analytical modelling of aerosol mass spectra. *Atmos. Chem. Phys.* **2007**, *7* (6), 1503–1522.
- (22) Odum, J. R.; Jungkamp, T. P. W.; Griffin, R. J.; Forstner, H. J. L.; Flagan, R. C.; Seinfeld, J. H. Aromatics, reformulated gasoline, and atmospheric organic aerosol formation. *Environ. Sci. Technol.* **1997**, *31* (7), 1890–1897.
- (23) Seinfeld, J. H.; Pandis, S. N. *Atmospheric chemistry and physics: From air pollution to climate change*; Wiley: New York, 1998; pp 714–722.
- (24) Zhang, Q.; Anastasio, C. Free and combined amino compounds in atmospheric fine particles (PM_{2.5}) and fog waters from northern California. *Atmos. Environ.* **2003**, *37* (16), 2247–2258.
- (25) Aiken, G. R. *Humic substances in soil, sediment, and water: Geochemistry, isolation, and characterization*; Wiley: New York, 1985; pp xiii–692.
- (26) Takegawa, N.; Miyakawa, T.; Kawamura, K.; Kondo, Y. Contribution of selected dicarboxylic and omega-oxocarboxylic acids in ambient aerosol to the m/z 44 signal of an aerodyne aerosol mass spectrometer. *Aerosol Sci. Technol.* **2007**, *41* (4), 418–437.
- (27) Allan, J. D.; Delia, A. E.; Coe, H.; Bower, K. N.; Alfarra, M. R.; Jimenez, J. L.; Middenrook, A. M.; Drewnick, F.; Onasch, T. B.; Canagaratna, M. R.; Jayne, J. T.; Worsnop, D. R. A generalised method for the extraction of chemically resolved mass spectra from aerodyne aerosol mass spectrometer data. *J. Aerosol Sci.* **2004**, *35* (7), 909–922.
- (28) Huffman, J. A.; Aiken, A. C.; Docherty, K.; Ulbrich, I. M.; DeCarlo, P. F.; Jayne, J. T.; Onasch, T. B.; Trimborn, A.; Worsnop, D. R.; Ziemann, P. J.; Jimenez, J. L. Volatility of primary and secondary organic aerosols in the field contradicts current model representations. 2008, in preparation.
- (29) Johnston, M. V. Near real-time speciation of organic aerosols for source apportionment. EPA Atmospheric Science Progress Review Meeting, 2007.
- (30) Heaton, K. J.; Dreyfus, M. A.; Wang, S.; Johnston, M. V. Oligomers in the early stage of biogenic secondary organic aerosol formation and growth. *Environ. Sci. Technol.* **2007**, *41* (17), 6129–6136.
- (31) Duplissy, J.; Gysel, M.; Alfarra, M. R.; Dommen, J.; Metzger, A.; Prevot, A. S. H.; Weingartner, E.; Laaksonen, A.; Raatikainen, T.; Good, N.; Turner, S. F.; McFiggans, G.; Baltensperger, U. Cloud forming potential of secondary organic aerosol under near atmospheric conditions. *Geophys. Res. Lett.* **2008**, *35* (1), L03818.

ES703009Q

Supporting Information:

O/C and OM/OC Ratios of Primary, Secondary, and Ambient Organic Aerosols with a High Resolution Time-of-Flight Aerosol Mass Spectrometer

Allison C. Aiken, Peter F. DeCarlo, Jesse H. Kroll, Douglas R. Worsnop, J. Alex Huffman, Kenneth Docherty, Ingrid M. Ulbrich, Claudia Mohr, Joel R. Kimmel, Donna Sueper, Yele Sun, Qi Zhang, Achim Trimborn, Megan Northway, Paul J. Ziemann, Manjula R. Canagaratna, Timothy B. Onasch, Rami Alfarra, Andre S.H. Prevot, Josef Dommen, Jonathan Duplissy, Axel Metzger, Urs Baltensperger, and Jose L. Jimenez

Supporting Information includes 6 pages with 4 Tables and 2 Figures.

Table S-1. Laboratory standard aerosols used for calibration of the EA method with the HR-ToF-AMS: (a) aerosol standards, (b) amino acids, (c) fulvic acids, (d) summary.**(a)**

#	Class	Subclass	Name	Formula	MW
1	Hydrocarbon	Alkane	Hexadecane	C ₁₆ H ₃₄	226.27
2		PAH	Fluoranthene	C ₁₆ H ₁₀	202.08
3		PAH	Pyrene	C ₁₆ H ₁₀	202.08
4		PAH	Benzo[e]pyrene	C ₂₀ H ₁₂	252.09
5	Alcohol	Alkanol	1-Octadecanol	C ₁₈ H ₃₈ O	270.29
6		Alkanol	1-Eicosanol	C ₂₀ H ₄₂ O	298.32
7		Alkanol	1-Docosanol	C ₂₂ H ₄₆ O	326.35
8		Dialkanol	1,2-Tetradecanediol	C ₁₄ H ₃₀ O ₂	230.22
9		Phenol	Pyrogallol	C ₆ H ₆ O ₃	126.03
10		Sterol	Cholesterol	C ₂₇ H ₄₆ O	386.35
11	Carboxylic Acid	Alkanoic Acid	Decanoic Acid	C ₁₀ H ₂₀ O ₂	172.15
12		Alkanoic Acid	Pentadecanoic Acid	C ₁₅ H ₃₀ O ₂	242.22
13		Alkanoic Acid	Hexadecanoic Acid	C ₁₆ H ₃₂ O ₂	256.24
14		Alkanoic Acid	Stearic Acid	C ₁₈ H ₃₆ O ₂	284.27
15		Alkenoic Acid	Oleic Acid	C ₁₈ H ₃₄ O ₂	282.26
16		Dicarboxylic Acid	Glutaric Acid	C ₅ H ₈ O ₄	132.04
17		Dicarboxylic Acid	Adipic Acid	C ₆ H ₁₀ O ₄	146.06
18		Dicarboxylic Acid	Undecanedioic Acid	C ₁₁ H ₂₀ O ₄	216.14
19		Hydroxy-carboxylic Acid	15-Hydroxypentadecanoic Acid	C ₁₅ H ₃₀ O ₃	258.22
20		Hydroxy-carboxylic Acid	16-Hydroxyhexadecanoic Acid	C ₁₆ H ₃₂ O ₃	272.24
21	Aldehyde	Alkanal	Nonyl Aldehyde	C ₉ H ₁₈ O	142.14
22	Ester	Phthalate	Diethyl Phthalate	C ₂₄ H ₃₈ O ₄	390.28
23		Alkanoate	Diethyl Sebacate	C ₂₆ H ₅₀ O ₄	426.37
24	Peroxide	Acyl Peroxide	Lauroyl Peroxide	C ₂₄ H ₄₆ O ₄	398.34
25		Acyl(Aroyl) Peroxide	Benzoyl Peroxide	C ₁₄ H ₁₀ O ₄	242.06
26	Anhydride	Alkyl Anhydride	Heptanoic Acid, anhydride	C ₁₄ H ₂₆ O ₃	242.19
27		Cyclic Anhydride	Glutaric Anhydride	C ₅ H ₆ O ₃	114.03
28	Carbohydrate	Monosaccharide	Levoglucosan	C ₆ H ₁₀ O ₅	162.05
29	Amine	Amino Acid	4-aminobenzoic acid	C ₇ H ₇ NO ₂	137.05
30		Amino Anhydride	N-methylisatioc Anhydride	C ₉ H ₇ NO ₃	177.04
31		Alkaloid	quinine	C ₂₀ H ₂₄ N ₂ O ₂	324.18
32	Amide	Alkyl Amide	bis-acrylamide	C ₇ H ₁₀ N ₂ O ₂	154.07
33	Nitro Aromatics	Nitro Phenol	3-Methyl-4-nitrophenol	C ₇ H ₇ NO ₃	153.04
34		Hydrazine Derivative	2,4-Dinitrophenylhydrazine	C ₆ H ₆ N ₄ O ₄	198.04
35	Pyridine Derivative	Cyclic Acid	Nicotinic Acid (Niacin)	C ₆ H ₅ NO ₂	123.03

(b)

#	Compound	Common Name	Abbreviation	Formula	MM
1	Methylammonium chloride	Methylamine hydrochloride	MMA(HCl)	CH ₃ NH ₂ (HCl)	31.04(35.98)
2	2-Aminoethanol hydrochloride	Ethanolamine hydrochloride	MEA(HCl)	C ₂ H ₇ NO (HCl)	61.05(35.98)
3	Aminoacetic acid	Glycine	Gly	C ₂ H ₅ NO ₂	75.03
4	2-aminopropanoic acid	Alanine	Ala	C ₃ H ₇ NO ₂	89.05
5	4-aminobutanoic acid	Aminobutyric acid	GABA	C ₄ H ₉ NO ₂	103.06
6	2-amino-3-methyl-butanoic acid	Valine	Val	C ₅ H ₁₁ NO ₂	117.08
7	2-amino-4-methyl-pentanoic acid	Leucine	Leu	C ₆ H ₁₃ NO ₂	131.10
8	2-amino-3-methylpentanoic acid	Isoleucine	Ile	C ₆ H ₁₃ NO ₂	131.10
9	2-Amino-3-hydroxybutanoic acid	Threonine	Thr	C ₄ H ₉ NO ₃	119.06
10	2-amino-3-hydroxypropanoic acid	Serine	Ser	C ₃ H ₇ NO ₃	105.04
11	2-aminopentanedioic acid	Glutamic Acid	Glu	C ₅ H ₉ NO ₄	147.05
12	2-aminobutanedioic acid	Aspartic Acid	Asp	C ₄ H ₇ NO ₄	133.04
13	2-amino-3-carbamoyl-propanoic acid	Asparagine	Asn	C ₄ H ₈ N ₂ O ₃	132.05
14	2,5-diaminopentanoic acid hydrochloride	Ornithine hydrochloride	Orn(HCl)	C ₅ H ₁₂ N ₂ O ₂ (HCl)	132.09(35.98)
15	2-Amino-3-phenyl-propanoic acid	Phenylalanine	Phe	C ₉ H ₁₁ NO ₂	165.08
16	2-Amino-3-(4-hydroxyphenyl)-propanoic acid	Tyrosine	Tyr	C ₉ H ₁₁ NO ₃	181.07
17	2-Amino-3-(1H-indol-3-yl)-propionic acid	Tryptophan	Trp	C ₁₁ H ₁₂ N ₂ O ₂	204.09
18	2-amino-4-(methylsulfanyl)-butanoic acid	Methionine	Met	C ₅ H ₁₁ NO ₂ S	149.05
19	2-Aminobutyric acid	2-Aminobutyric acid	<i>n/a</i>	C ₄ H ₉ NO ₂	103.06
20	2-amino-4-(methylsulfanyl)-butanoic acid sulfoxide	Methionine Sulfoxide	Met(SO)	C ₅ H ₁₁ NO ₃ S	165.05

(c)

#	Compound	Class	Formula
1	Suwannee River I	FA Standard	1S101F
2	Suwannee River II	FA Standard	2S101F
3	Nordic Lake	FA Reference	1R105F
4	Waskish Peat	FA Reference	1R107F

(d)

Category	#	Published
Aerosol Standards	35	Aiken et al., 2007 (14)
Amino Acids	20	Sun and Zhang, 2008 (23)
Fulvic Acids	4	
Total	59	

Table S-2. Sensitivity Analysis for the effect of the use of half of the water signal as organic-originated signal for the fulvic acid data. (Δ slope = Percent change in the calibration slope, Avg Abs Err = average absolute value of the error as described in the text).

	O/C				H/C			
	All Samples			FA	All Samples			FA
	Slope	Δ Slope	Avg Abs Error	Avg Abs Error	Slope	Δ Slope	Avg Abs Error	Avg Abs Error
Current (FA, 1/2 Water)	0.75		31%	4%	0.91		10%	24%
FA (No Water)	0.73	-3%	32%	18%	0.91	0%	9%	6%
FA (All Org Water)	0.77	3%	32%	14%	0.92	1%	12%	42%

Table S-3. Changes to the standard organic fragmentation table (frag_organic) used in the AMS software (SQUIRREL).

m/z	Standard (frag_organic)	New (frag_organic_new)
18	1*frag_organic[44]	0.225*frag_organic[44]
28	0	frag_organic[44]

Table S-4. Direction (+/-) of the potential remaining biases in the EA method for O/C, H/C and N/C. A “+” means that this effect is likely to create a positive bias in a given quantity, while a “-“ indicates a likely negative bias.

	O/C	H/C	N/C
E_b	-	+	?
RIE	-	+	?
$N_xO_y^+$ from organic nitrates (counted as inorganic nitrate)	-	0	-
$S_xO_y^+$ from organic sulfates (counted as inorganic sulfate)	-	0	0

Figure S-1. Elemental HRMS signals summed to UMR for the average Mexico City ground data.

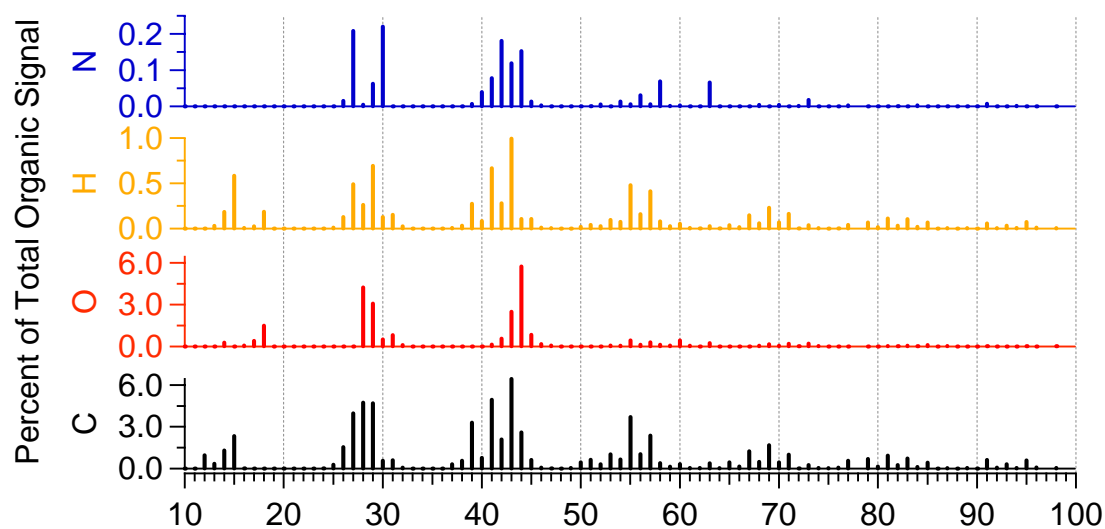


Figure S-2. Scatter plot of percent CO_2^+/OA signal vs. atomic O/C from ground and aircraft ambient MILGARO measurements, fit by linear regression ($\pm 95\%$ CI) and weighting ground and aircraft data equally.

